Supporting Information for

New Insight into Impact of Humidity on Direct Air Capture by SIFSIX-3-Cu

Behrouz Bayati[1,2], Fatemeh Keshavarz[3], Nima Rezaei[4], Sohrab Zendehboudi[2]*, Bernardo Barbiellini[3,5]

[1]Department of Chemical Engineering, Ilam University, Ilam, 6939177111 Iran

[2]Department of Process Engineering, Memorial University, St. John's, NL, A1C 5S7 Canada

[3]Department of Physics, School of Engineering Science, LUT University, FI-53850 Lappeenranta, Finland

[4]Department of Separation Science, School of Engineering Science, LUT University, FI-53850 Lappeenranta, Finland

[5]Department of Physics, Northeastern University, Boston, Massachusetts 02115, United States

*Email address of corresponding author: szendehboudi@mun.ca

S1. Computational Details

The Density Functional Theory (DFT) calculations are performed using the Vienna Ab Initio Simulation Package (VASP), version 6.3.0.[1] Because of the success of the Perdew−Burke−Ernzerhof (PBE)[2] Generalized Gradient Approximation (GGA) in describing the electronic structure of SIFSIX-3-Cu,[3-7] we employ the PBE exchange correlation functional along with the projector augmented wave (PAW) pseudopotentials.[8] The PAW parameters are extracted from the VASP POTCAR library for N (s^2p^3), C (s^2p^2), H, Cu_pv (d^{10} p^1), F (s^2p^5), Si (s^2p^2), and O (s^2p^4). Periodic boundary condition is applied to the unit cell of SIFSIX-3-Cu[9] in all directions, and spin polarization (a doublet ground spin state) is considered.[4] To include long-range dispersion effects on the calculations, the DFT-D3 van der Waals corrections with Becke-Jonson damping are applied.[10,11] To decrease the computational errors, the "accurate" precision mode is used. The convergence limit of the self-consistent electronic structure calculations is set to 10^{-5} eV. The partial electron occupancies of each orbital are treated with 0.03 eV Gaussian smearing.

According to our calibration results reported in Table S1, a Monkhorst-Pack grid of 4 × 4 × 4 (Γ-point only) is used to sample the Brillouin zone, and a kinetic energy cutoff of 500 eV is used in expansion of the Kohn-Sham wave functions. During the optimization of the geometries, only the atomic coordinates are modified until the force on each atom is less than 0.05 eV $Å^{-1}$. Our additional calculations on optimization of the unit cell's shape and volume (see Table S2) show that the selected computational parameters can reproduce the experimental unit cell with less than 0.6% error.

To evaluate the adsorption of CO_2 and H_2O onto the SIFSIX-3-Cu structure, the adsorbate molecules are placed at random positions, and the structure and electronic energy are relaxed. To calculate the energy of the isolated gas molecules (the SIFSIX-3-Cu systems), Gaussian smearing is increased to 0.10 eV. In all calculations, the system size is set equal to the unit cell dimensions ($a = b = 6.9186$ Å, $c = 7.9061$ Å)[9].

Table S1. Effect of various parameters on optimization of the electronic energy (*E*) and geometry of SIFSIX-3-Cu.*

E_{cut} (eV)	ISIF	KPOINTS	*E* (eV)	CPU time (s)
500	2	111	-142.7136741	8913.337
500	2	222	-142.7986283	10187.529
500	2	223	-142.7987461	9080.726
500	2	333	-142.8105576	10089.657
500	***2***	***444***	***-142.8101817***	***11054.34***
450	2	444	-142.8132342	10738.166
550	2	444	-142.8162111	10876.07
500	3	444	-142.8288571	12072.502
500	4	444	-142.8103208	11355.394

* E_{cut}: Cut-off energy; ISIF=2: only the atomic positions are optimized; ISIF=3: the atomic positions, cell shape, and cell volume are optimized; ISIF=4: the atomic positions and cell shapes are optimized; KPOINTS: the Bloch vectors (*k* points) used to sample the Brillouin zone; and 111 represents a 1 × 1 × 1 sampling space.

Table S2. Comparison of the calculated and experimental cell parameters. [9]*

	a, *b*	*c*	MEA (%)
Exp.	6.9186	7.9061	-
ISIF = 3	6.8632 (0.36)	7.8777 (0.58)	0.58
ISIF = 4	6.9129 (0.08)	7.9191 (0.16)	0.12

* The values in parentheses are the absolute errors (%) relative to the experimental parameters; and MEA stands for the mean absolute error. ISIF=3: the atomic positions, cell shape, and cell volume are optimized; and ISIF=4: the atomic positions and cell shapes are optimized.

S2. Results and Discussion

The adsorption modes and energies obtained from DFT simulations are presented in Figure S1. As shown, water adsorbs onto SIFSIX-3-Cu in five different configurations with varying adsorption energies. CO_2 can be adsorbed in just one adsorption mode.

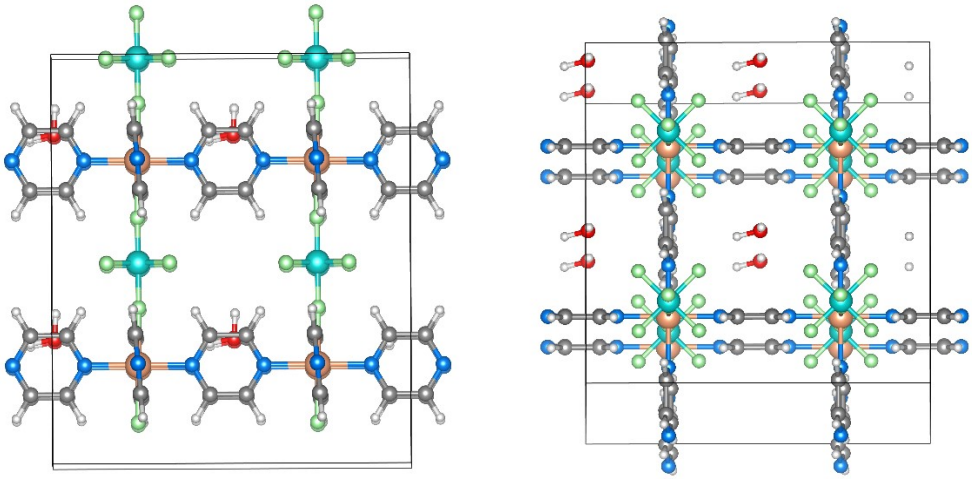

E_{ad}: -83.4 kJ mol^{-1}

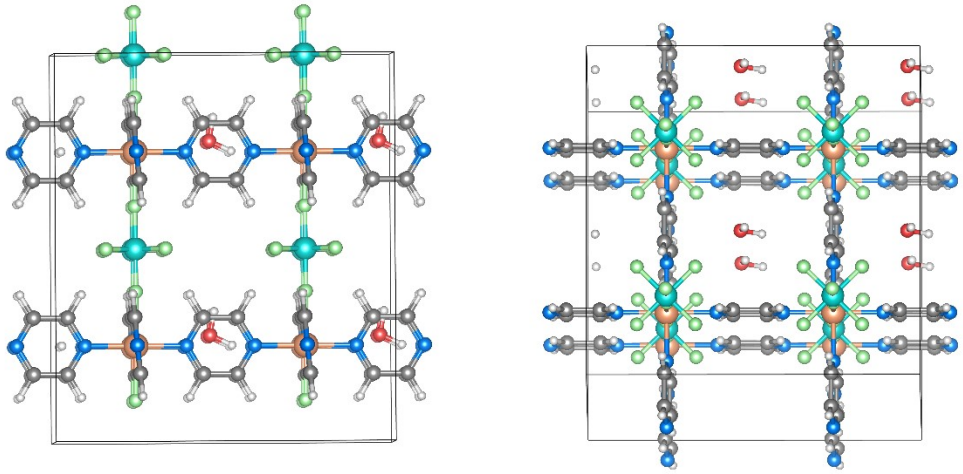

E_{ad}:-81.4 kJ mol^{-1}

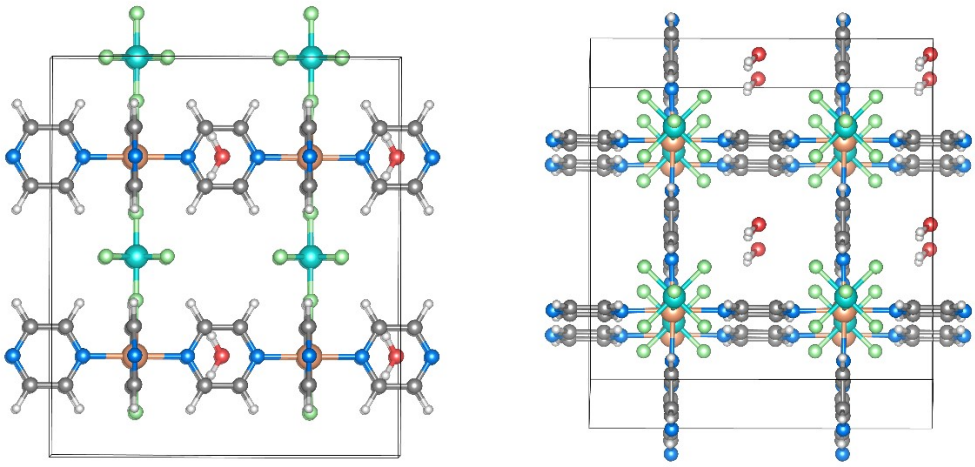

E_{ad}: -79.7 kJ mol^{-1}

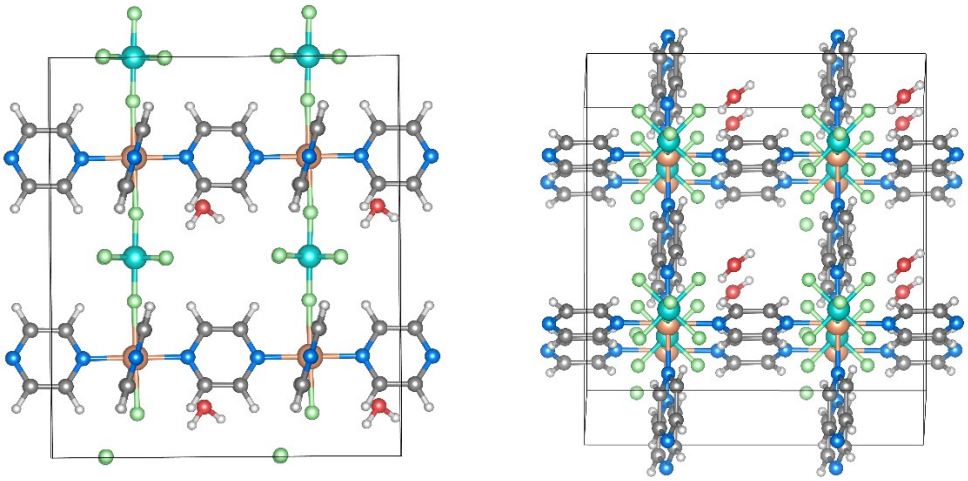

E_{ad}: -105.3 kJ mol^{-1}

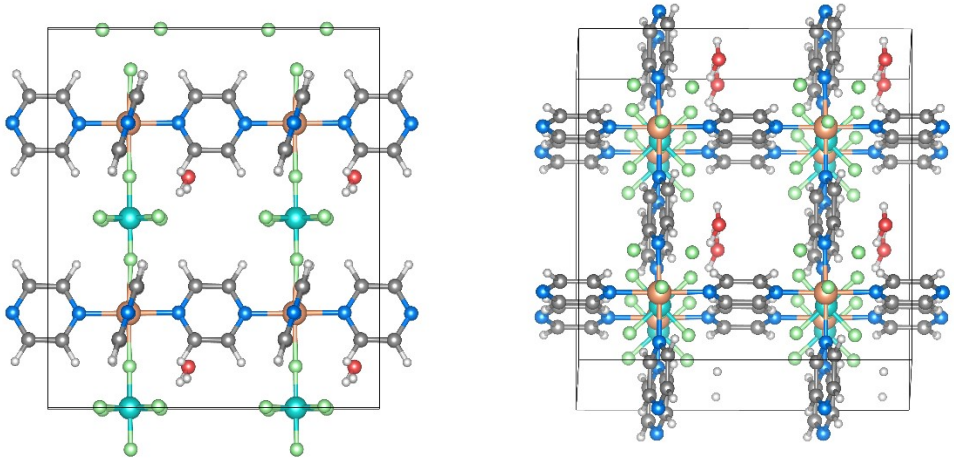

E_{ad}: -106.9 kJ mol^{-1}

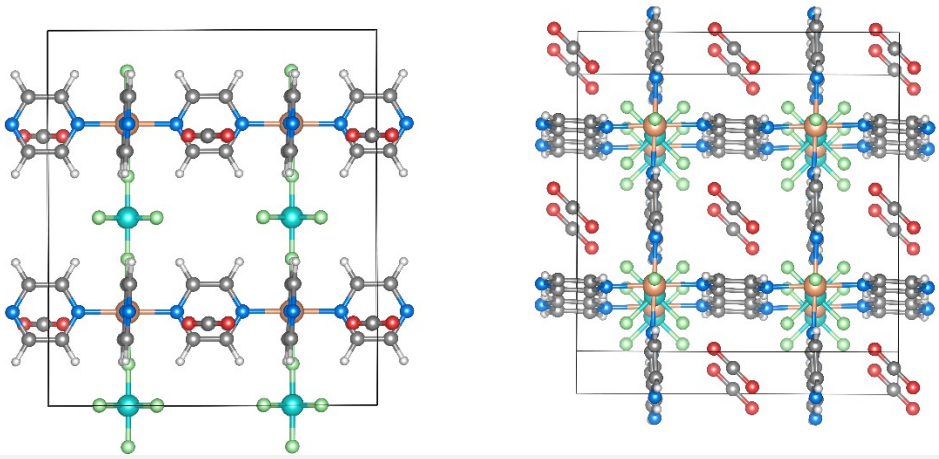

E_{ad}: -67.9 kJ mol^{-1}

Figure S1. The H_2O and CO_2/SIFSIX-3-Cu adsorption modes and energies (0 K). The unit cell is duplicated (2 × 2 × 2) to show the binding modes more precisely.

Consistent with the DFT results, the distribution of the CO_2 and H_2O molecules in SIFSIX-3-Cu obtained from MD simulations at two different molar ratios and room conditions (Figures S2 and S3) demonstrate the preference of H_2O adsorption and the diverse adsorption modes of H_2O.

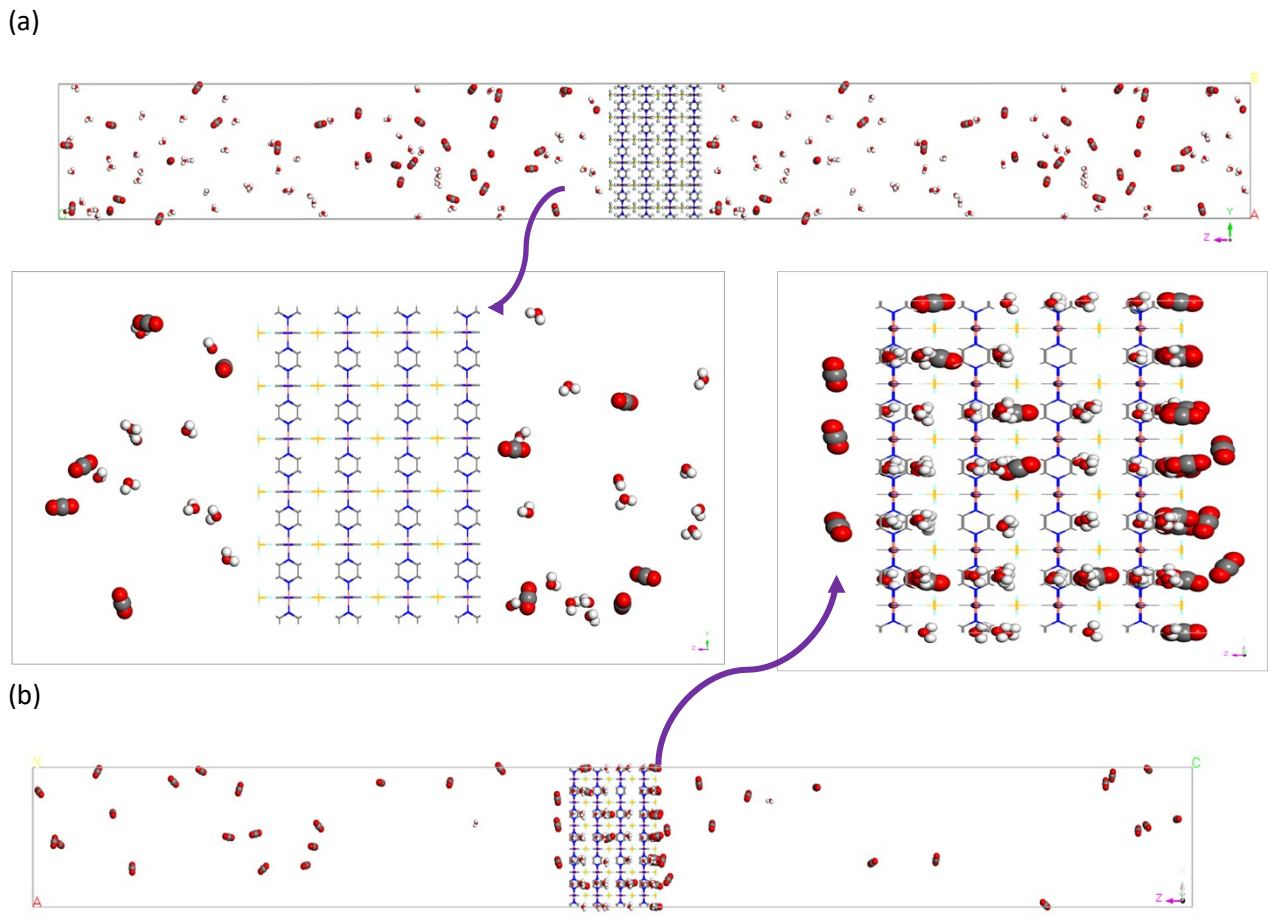

Figure S2. (a) Initial state and (b) final state of MD results for adsorption and distribution onto SIFSIX-3-Cu for a gas mixture with the H_2O:CO_2= 60:30 molar ratio, at 298 K and 1 atm.

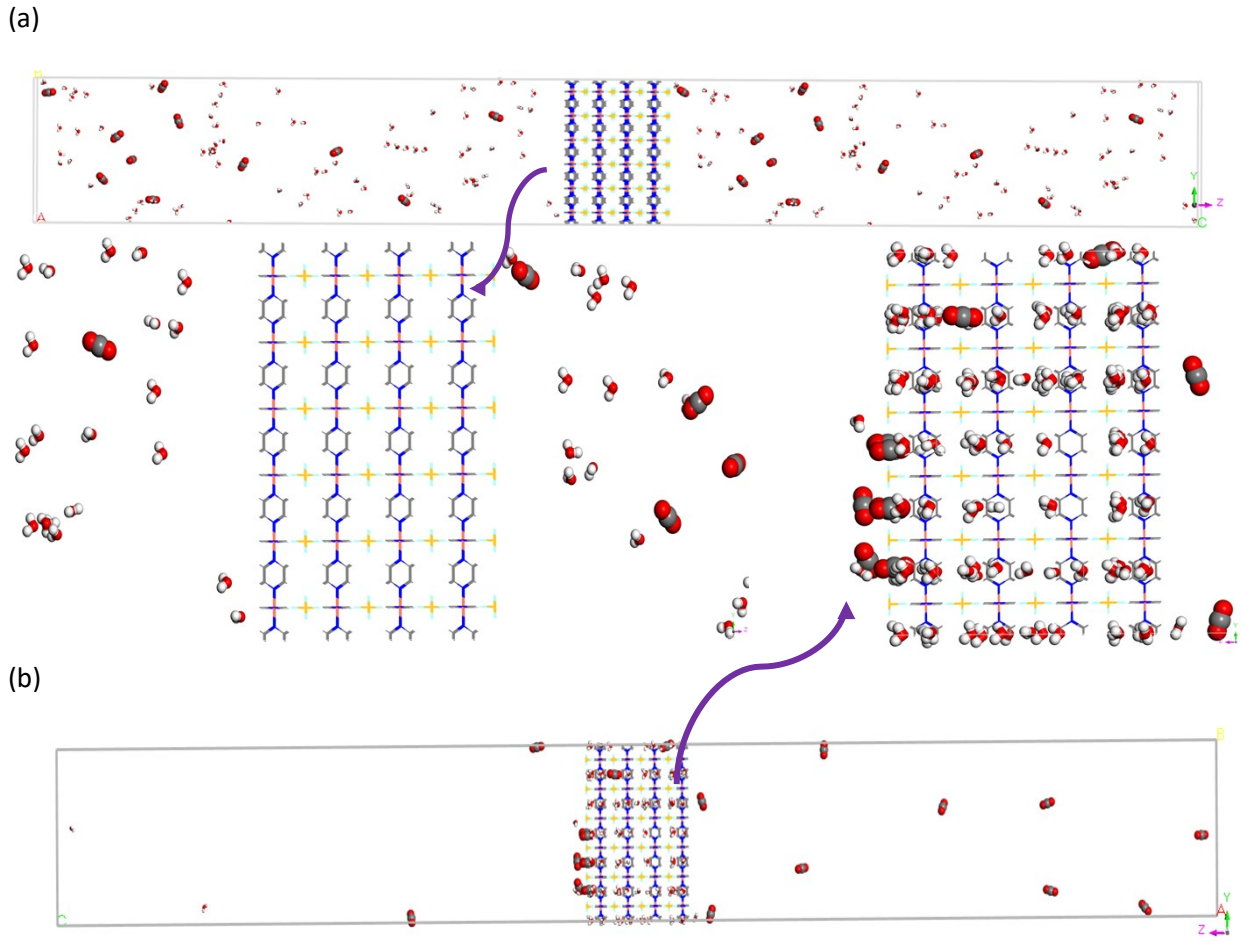

Figure S3. (a) Initial state and (b) final state of MD results for adsorption and distribution onto SIFSIX-3-Cu for a gas mixture with the H_2O:CO_2= 80:10 molar ratio, at 298 K and 1 atm.

Figure S4 represents the movement of the mass transfer zone along the adsorption tower through a simple schematic manner. As H_2O has a high tendency to adsorb on SIFSIX-3-Cu, CO_2 molecules are unable to be adsorbed in the H_2O mass transfer zone. Consequently, CO_2 molecules are adsorbed after the mass transfer zone of H_2O.

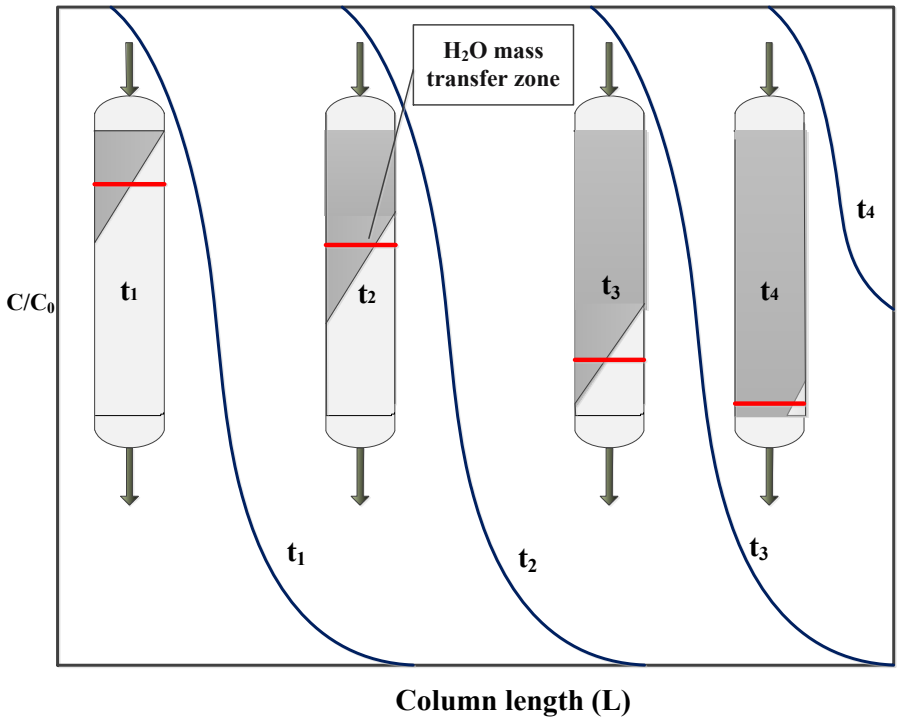

Figure S4. The evolution of H_2O-saturated mass transfer zone along the height of adsorption packed bed column. [12]

References

(1) G. Kresse, J. Furthmüller, Efficiency of Ab-Initio Total Energy Calculations for Metals and Semiconductors Using a Plane-wave Basis Set. *Comput. Mater. Sci.* 1996, *6*, 15-50.

(2) J. P. Perdew, K. Burke, M. Ernzerhof, Generalized Gradient Approximation Made Simple. *Physical Rev. Lett.* 1996, *77*, 3865.

(3) A. Ziaee, D. Chovan, M. Lusi, IV, J. J. Perry, M. J. Zaworotko, S. A. M. Tofail, Theoretical Optimization of Pore Size and Chemistry in SIFSIX-3-M Hybrid Ultramicroporous Materials. *Cryst. Growth Des.* 2016, *16*, 3890-3897.

(4) K. A. Forrest, T. Pham, S. K. Elsaidi, M. H. Mohamed, P. K. Thallapally, M. J. Zaworotko, B. Space, Investigating CO_2 Sorption in SIFSIX-3-M (M= Fe, Co, Ni, Cu, Zn) through Computational Studies. *Cryst. Growth Des.* 2019, *19*, 3732-3743.

(5) W. G. Guimarães, G. F. de Lima, Investigating Greenhouse Gas Adsorption in MOFs SIFSIX-2-Cu, SIFSIX-2-Cu-i, and SIFSIX-3-Cu through Computational Studies. *J. Mol. Model.* 2020, *26*, 1-11.

(6) L. U. Xiaoqing, W. A. N. G. Maohuai, Theoretical Investigation on Adsorption and Separation of CO_2/N_2 in Hybrid Ultramicroporous Materials. *J. Inorg. Mater.* 2020, *35*, 469.

(7) J. Yuan, X. Liu, X. Li, J. Yu, Computer Simulations for the Adsorption and Separation of $CH_4/H_2/CO_2/N_2$ Gases by Hybrid Ultramicroporous Materials. *Mater. Today Commun.* 2021, *26*, 101987.

(8) G. Kresse, D. Joubert, From Ultrasoft Pseudopotentials to the Projector Augmented-wave Method. *Phys. Rev. B* 1999, *59*, 1758.

(9) O. Shekhah, Y. Belmabkhout, Z. Chen, V. Guillerm, A. Cairns, K. Adil, M. Eddaoudi, Made-to-order Metal-Organic Frameworks for Trace Carbon Dioxide Removal and Air Capture. *Nature Commun.* 2014, *5*, 1-7.

(10) S. Grimme, J. Antony, S. Ehrlich, H. Krieg, A Consistent and Accurate Ab Initio Parametrization of Density Functional Dispersion Correction (DFT-D) for the 94 Elements H-Pu. *J. Chem. Phys.* 2010, *132*, 154104.

(11) S. Grimme, S. Ehrlich, L. Goerigk, Effect of the Damping Function in Dispersion Corrected Density Functional Theory. *J. Comput. Chem.* 2011, *32*, 1456-1465.

(12) A. Gabelman, Adsorption basics: part 1. *Chemical Engineering Progress* 2017, *113* (7), 48-53.